International Journal of Heat and Technology
Vol. 42, No. 3, June, 2024, pp. 905-916
Journal homepage: http://iieta.org/journals/ijht

Pyrolysis Characteristics of Construction Waste and Its Application in Low-Temperature Thermal Cycle Systems

Boyi Yao[1], Qin Li[2], Chunshui Huang[3*]

[1] Zhejiang Communications Construction Group Co., Ltd, Hangzhou 310000, China
[2] Henan Xuwei Ring Expressway Co., Ltd, Zhengzhou 450016, China
[3] College of Civil Engineering, Xuchang University, Xuchang 461000, China

Corresponding Author Email: 12015042@xcu.edu.cn

https://doi.org/10.18280/ijht.420319

Received: 26 January 2024
Revised: 9 April 2024
Accepted: 20 May 2024
Available online: 27 June 2024

Keywords:
construction waste, pyrolysis reaction, low-temperature thermal cycle system, thermodynamic performance, resource utilization

ABSTRACT

The urbanization process generates a substantial amount of construction waste, and traditional disposal methods lead to environmental pollution and resource wastage. There is an urgent need to develop more efficient and environmentally friendly treatment technologies. This paper investigates the pyrolysis characteristics of construction waste and its application in low-temperature thermal cycle systems. First, the pyrolysis reaction mechanism of construction waste is analyzed through experiments and simulations, revealing the decomposition patterns and reaction mechanisms of various components during pyrolysis. Secondly, the thermodynamic performance of construction waste in low-temperature thermal cycle systems is evaluated to explore its feasibility and application prospects in practical engineering. The research results indicate that the pyrolysis of construction waste can effectively reduce waste volume and produce high-value-added products. The low-temperature thermal cycle system shows promising potential in terms of energy utilization efficiency and economic viability. This study provides a theoretical foundation for the treatment and resource utilization of construction waste and is significant for promoting green building and sustainable development.

1. INTRODUCTION

Construction waste is generated during construction, demolition, and renovation processes in the construction industry. Its quantity is enormous and its composition is complex [1-3]. With the acceleration of urbanization and the increase in construction activities, the treatment and utilization of construction waste have become urgent issues [4, 5]. Traditional methods such as landfill and incineration not only waste resources but also cause severe environmental pollution [6-8]. Therefore, how to effectively treat and resourcefully utilize construction waste has become one of the research hotspots.

The study of the pyrolysis characteristics of construction waste and its application in low-temperature thermal cycle systems is of great significance [9-11]. Pyrolysis is an effective technology that can convert organic waste into renewable energy. By pyrolyzing construction waste, not only can the volume of waste be reduced, but high-value-added products for energy production can also be obtained [12, 13]. Additionally, applying pyrolysis products to low-temperature thermal cycle systems helps improve energy utilization efficiency, promote the development of a circular economy, and reduce dependence on traditional fossil energy, which has broad application prospects [14].

Current research methods mainly focus on high-temperature pyrolysis and its application in high-temperature thermal systems. However, high-temperature pyrolysis involves significant energy loss and high equipment costs, limiting its practical application [15-17]. Moreover, many studies have failed to analyze the pyrolysis reaction mechanism of construction waste in depth, lacking systematic research on low-temperature thermal cycle systems [18-20]. Existing methods have obvious deficiencies in energy efficiency and economic viability, urgently requiring the development of new research ideas and technical means.

The main research content of this paper is divided into two parts: first, to analyze the pyrolysis reaction mechanism of construction waste, revealing the decomposition patterns and reaction mechanisms of various components during pyrolysis through experimental and simulation studies; second, to analyze the thermodynamic performance of the low-temperature thermal cycle system for construction waste, evaluating its energy utilization efficiency and economic benefits, and exploring its feasibility and application prospects in practical engineering. This study not only enriches the theoretical system of construction waste treatment and resource utilization but also provides a scientific basis for the optimal design of low-temperature thermal cycle systems, having significant theoretical and practical significance for promoting green building and sustainable development.

2. ANALYSIS OF PYROLYSIS REACTION MECHANISM OF CONSTRUCTION WASTE

Pyrolyzable construction waste mainly includes various organic and inorganic waste generated during construction, renovation, and demolition processes. These wastes are complex in composition, but most of them have a certain pyrolysis potential. Wood waste, plastic waste, rubber waste, paper waste, fabric waste, and synthetic material waste are some common types of pyrolyzable construction waste. The wood used in construction and the waste generated during its processing, such as wood chips, sawdust, old wood boards, and wooden furniture. These wood wastes contain rich organic components, which can be converted into valuable products such as bio-oil, syngas, and charcoal through pyrolysis. Plastic products in building materials include PVC pipes, insulation materials, plastic films, and packaging materials. Plastic waste can be decomposed into fuel oil and gas during pyrolysis, having high utilization value for pyrolysis products. Rubber products used in construction, such as waterproof materials, floor mats, and seals, can produce oils and gases through pyrolysis, and some residues can be used for recycled rubber products. Paper waste includes packaging paper on construction sites, discarded cardboard, and wallpaper used during renovation. These paper wastes contain high cellulose and hemicellulose components, which can be converted into biochar and fuel gas through pyrolysis. Various fabric materials used in the construction process, such as carpets, curtains, and decorative fabrics, generally contain a lot of organic components, and the pyrolysis products are mainly liquid fuels and gases. Various synthetic materials used in construction, such as polyurethane foam, glass fiber reinforced plastic (GRP), and polystyrene (PS) boards. The pyrolysis of these materials can produce synthetic oil and gas, having a certain heat recovery utilization value. Figure 1 below shows the types of construction waste and products generated by pyrolysis.

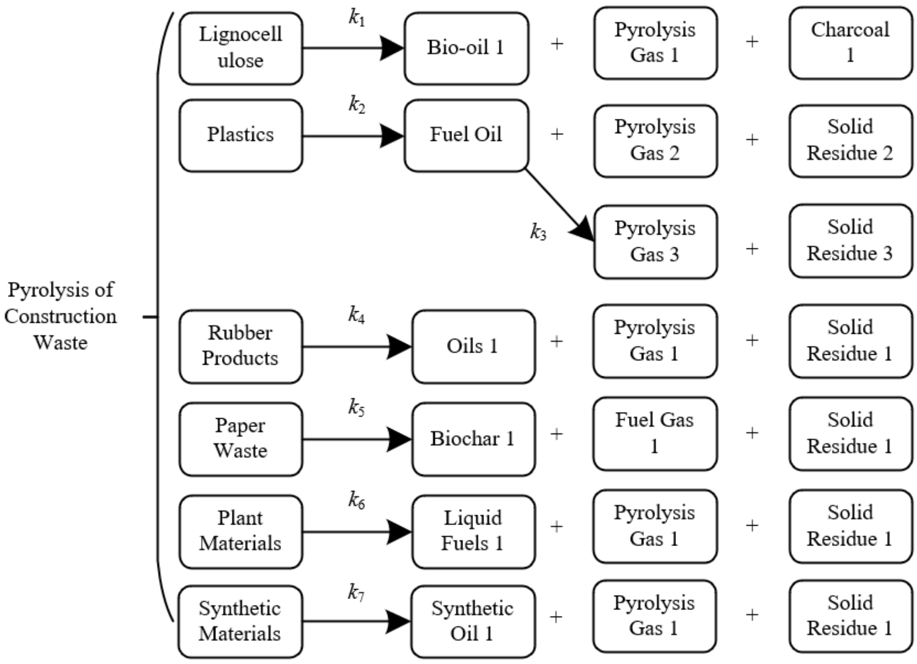

Figure 1. Types of construction waste and products generated by pyrolysis

In studying the pyrolysis reaction mechanism of construction waste, we conducted an in-depth analysis of the pyrolysis process using a staged reaction model. This model assumes that the reactant of the pyrolysis reaction is a single entity. By reaction time or temperature, the pyrolysis process of construction waste can be divided into four main temperature intervals, each representing a different reaction stage with unique kinetic parameters. Within each temperature interval, the relationship between $IN(\int^{\beta}_{0}(d\beta/H(\beta))/S^2)$ and $1/S$ is linear, as shown by the curve given in Figure 2 below. These stages are: the low-temperature initial stage (100-300℃), mainly involving the release of moisture and some low-temperature volatiles; the medium-temperature rapid decomposition stage (300-500℃), where a large amount of organic matter begins to decompose, producing gas, liquid, and solid products; the high-temperature stable decomposition stage (500-700℃), where the decomposition of volatile substances tends to stabilize and solid residues gradually decrease; and the ultra-high-temperature complete decomposition stage (above 700℃), where the remaining solid substances further decompose, mainly producing gas and a small amount of residue.

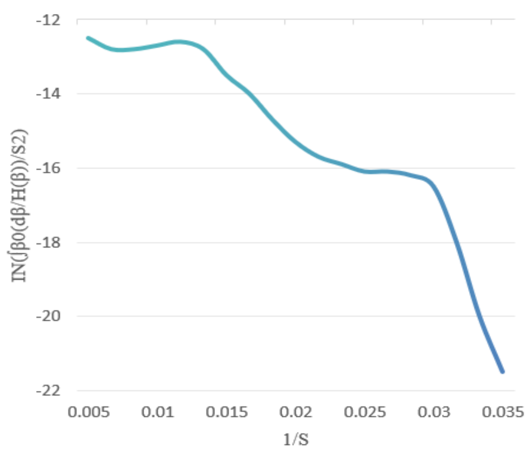

Figure 2. Curve of $IN(\int^{\beta}_{0}(d\beta/H(\beta))/S^2)$ versus $1/S$

The rate equation of the pyrolysis reaction in this model can be expressed as:

$$\begin{cases} \frac{\partial \beta}{\partial s} = X_{S_1\sim S_2} \exp\left(-\frac{R_{S_1\sim S_2}}{ES}\right) H_{S_1\sim S_2}(\beta) S_1 \leq S \leq S_2 \\ \frac{\partial \beta}{\partial s} = X_{S_2\sim S3} \exp\left(-\frac{R_{S_2\sim S_3}}{ES}\right) H_{S_2\sim S_3}(\beta) S_2 \leq S \leq S_3 \end{cases} \tag{1}$$

In the analysis of the pyrolysis reaction mechanism of construction waste, using the Distributed Activation Energy Model (DAEM) can more accurately describe the kinetic parameters at different stages. The pyrolysis process of construction waste is complex, with significant differences in the decomposition behavior and reaction rates of different components. Through the DAEM, the activation energy distribution at different reaction stages can be analyzed, which is important for understanding the decomposition mechanisms of various components during the pyrolysis of construction waste. Unlike traditional methods that regard the activation energy and pre-exponential factor as constants, the DAEM allows the activation energy to vary with the reaction progress, making the model closer to reality. The model assumes the reaction mechanism function as $H(\beta)=(1-\beta)^v$ and represents the difference in activation energy using a continuous distribution function $g(E)$. If the difference in activation energy is represented by a continuous distribution function $h(R)$, the DAEM equation is as follows:

$$\begin{cases} \frac{\partial \beta}{\partial s} = \int_0^\infty \frac{X\exp\left(-\frac{R}{ES}\right)}{\left[1-(-v)\int_0^s X\exp\left(-\frac{R}{ES}\right)ds\right]^{v/1-v}} h(R)dR \quad v \neq 1 \\ \frac{\partial \beta}{\partial s} = \int_0^s X\exp\left[-\frac{R}{ES} - \int_0^s X\exp\left(-\frac{R}{ES}\right)ds\right] h(R)dR \quad v = 1 \end{cases} \tag{2}$$

Although the DAEM is theoretically more precise, its equation includes two integrals over time t and activation energy E, making the solution complex and requiring approximate methods or computer software to solve.

The pyrolysis process of construction waste may involve multiple parallel and continuous reactions that occur simultaneously in a short period, forming complex pyrolysis behavior. Additionally, the pyrolysis behavior of different materials varies significantly within different temperature intervals. For example, wood starts to decompose at lower temperatures, while plastic undergoes significant pyrolysis reactions at higher temperatures. Moreover, construction waste often contains various impurities, which may alter the pathways and rates of pyrolysis reactions, making the reaction mechanism more complex. This complexity necessitates the analysis of the apparent pyrolysis mechanism, deducing the kinetic parameters and mechanism functions that reflect the overall pyrolysis behavior through experimental data and mathematical model fitting. Since different stages of the pyrolysis reaction of construction waste may correspond to different mechanism functions, the study needs to select or determine the most appropriate mechanism function based on the specific pyrolysis characteristics and reaction laws. The low-temperature initial stage may involve complex physical adsorption and initial volatilization processes, suitable for different mechanism models; the medium-temperature rapid decomposition stage may be more suitable for first-order reaction models or complex decomposition mechanism functions; and the high-temperature stable decomposition stage may lean towards a simple first-order reaction model or other mechanism functions more suitable for high-temperature reactions. Specifically, integrating the conversion rate of reactants yields:

$$\int_0^\beta \frac{d\beta}{H(\beta)} = \int_0^s j ds = js + y \tag{3}$$

By substituting different mechanism functions into the above equation and plotting the relationship between $\int^\beta_0(d\beta/H(\beta))$ and s, the experimental values of $\int^\beta_0(d\beta/H(\beta))$ at different times are compared with the regression line, and the one with the highest fitting degree is the best mechanism function for the pyrolysis reaction process of construction waste. Additionally, rearranging Eq. (2) yields:

$$IN\int_0^\alpha \frac{f\beta}{d(\beta)} = -IN\alpha + IN\left(\frac{XR}{E}\right) + IN[O(a)] \tag{4}$$

Conducting thermogravimetric experiments on the pyrolysis reaction of construction waste at different heating rates, substituting the β values at the same temperature into the formula reveals that the value of $IN(XE/R)+IN[o(a)]$ is constant. By combining the above equation with different pyrolysis reaction mechanism functions of construction waste and comparing the slope of the $IN\int^\beta_0[d\beta/H(\beta)]$ versus $IN\alpha$ curve approaching -1, the linear correlation of the curve can be further analyzed to obtain the best pyrolysis reaction mechanism for construction waste.

3. THERMODYNAMIC PERFORMANCE ANALYSIS OF LOW-TEMPERATURE THERMAL CYCLE SYSTEM FOR CONSTRUCTION WASTE

The traditional Rankine cycle mainly consists of four key components: an evaporator, an expander, a condenser, and a working fluid pump. The working fluid pump compresses and pressurizes the working fluid, which then enters the evaporator and exchanges heat with high-temperature exhaust gas, raising its temperature and evaporating it into gas. Subsequently, the high-temperature, high-pressure gaseous working fluid expands and does work in the expander, driving the generator to generate electricity. The low-pressure gaseous working fluid is condensed into liquid form in the condenser and returns to the working fluid pump, entering the next cycle. In this process, the working fluid absorbs energy from the heat source in the evaporator and releases energy in the expander, converting thermal energy into kinetic energy. Figure 3 shows the principle of the Rankine cycle. In the low-temperature thermal cycle system for construction waste, construction waste acts as a low-temperature heat source. Unlike the traditional Rankine cycle, its heat source temperature is relatively low. To improve system efficiency, a preheater and a regenerator are usually added to the system. The preheater is used to preheat the working fluid with the fluid returning from the condenser before it enters the evaporator, increasing the working fluid temperature and reducing the evaporator's heat load. The regenerator uses the residual heat of the low-pressure gaseous working fluid after expansion to further increase the initial temperature of the working fluid.

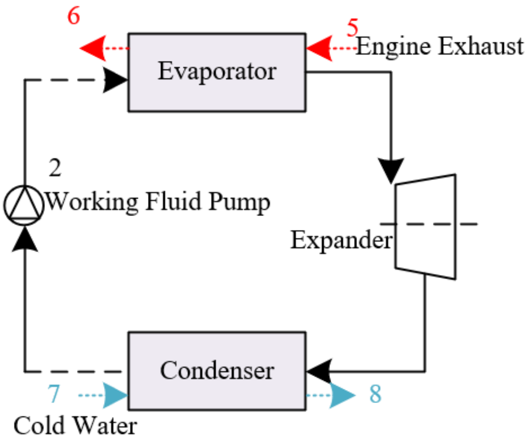

Figure 3. Principle of the Rankine cycle

Specifically, after being compressed and pressurized by the working fluid pump, the working fluid first enters the preheater, where it exchanges heat with the low-temperature liquid working fluid coming from the condenser. The preheated working fluid then enters the evaporator, where it exchanges heat with the residual heat released by the construction waste, raising its temperature and evaporating it into high-temperature, high-pressure gaseous working fluid. Subsequently, the gaseous working fluid expands and does work in the expander, driving the generator to generate electricity. After releasing energy, it enters the regenerator to exchange heat with the preheated working fluid. Finally, the low-pressure gaseous working fluid is condensed into liquid form in the condenser and re-enters the working fluid pump, completing a cycle.

This low-temperature thermal cycle system for construction waste based on the Rankine cycle not only fully utilizes the low-temperature residual heat in construction waste, improving energy utilization efficiency, but also reduces environmental pollution, having significant environmental benefits. By optimizing system design and reasonably configuring the preheater and regenerator, high-efficiency, low-cost energy conversion and recovery can be achieved while ensuring the system's thermodynamic performance, providing an effective technical approach for the treatment and resource utilization of construction waste.

3.1 Modeling and validation of the Rankine bottom cycle

As the low-temperature heat source for the system, construction waste has a relatively low and highly fluctuating heat source temperature. Therefore, when designing the thermal cycle system, special attention needs to be paid to optimizing the heat exchange process to ensure the system's efficient operation. The pinch point temperature difference analysis method is a core technology in the optimal design of process systems. By controlling the temperature difference between the working fluid and the heat source during the heat exchange process, this method makes their temperature changes more uniform and reduces energy loss. In the low-temperature thermal cycle system for construction waste based on the Rankine cycle, this method can effectively solve the heat exchange problem in the application of high-temperature heat sources in the traditional Rankine cycle, making the system more adaptable to the characteristics of low-temperature heat sources.

Specifically, in the model of the low-temperature thermal cycle system for construction waste, the inlet temperature and flow rate of the heat source are known. After setting the evaporation pressure and superheat degree, the thermodynamic parameters of the working fluid at each key point can be determined. Using the pinch point temperature difference analysis method, a reasonable pinch point temperature difference ΔS_{oo} can be set in the heat exchanger design to ensure maximum heat exchange efficiency between the working fluid and the construction waste heat source during the heating process. That is, the pinch point temperature difference analysis method ensures that the temperature changes of the working fluid in the preheater and evaporator are more matched with the temperature changes of the heat source, reducing irreversible losses during the heat exchange process. For example, in the preheater, through reasonable design, the temperature of the working fluid gradually increases in sync with the temperature changes of the heat source, avoiding large temperature difference zones and thus improving heat exchange efficiency. In the evaporator, by controlling the evaporation pressure and superheat degree, the evaporation process of the working fluid is more uniform, making full use of the residual heat from the construction waste. In addition, the pinch point temperature difference analysis method can also optimize the design of the regenerator. The regenerator utilizes the residual heat of the working fluid after expansion to preheat the working fluid before it enters the evaporator. The pinch point temperature difference analysis ensures that the heat exchange process in the regenerator is also efficient, further enhancing the overall energy efficiency of the system.

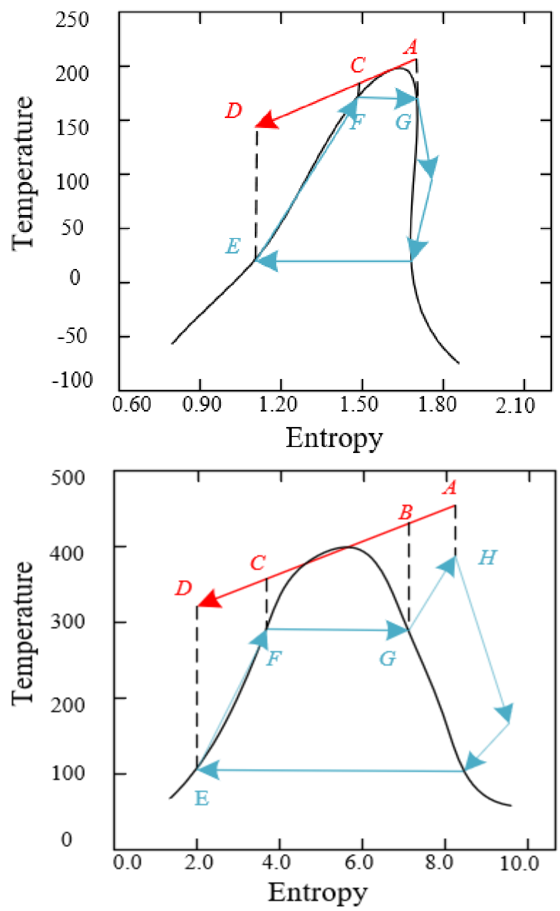

Figure 4. Temperature-entropy diagram of subcritical saturated cycle and subcritical superheated cycle

Figure 4 shows the temperature-entropy diagram of the subcritical saturated cycle and the subcritical superheated cycle. Assuming that in the low-temperature thermal cycle system model for construction waste, the inlet temperature and flow rate of the low-temperature heat source are known. After setting the evaporation pressure O_{MAX} and the superheat degree for the subcritical superheated cycle, the thermodynamic parameters at points *D*, *H*, and *G* of the working fluid can be determined. The establishment of the low-temperature thermal cycle system model for construction waste involves the following parts:

(1) In the initial stage of modeling, it is assumed that the pinch point temperature difference occurs at the saturation point *D* of the working fluid. At this point, the state parameters of the working fluid at the saturation point can be determined, including saturation temperature and pressure. Based on this assumption, the corresponding exhaust temperature can be preliminarily calculated.

$$S_Z = S_D + \Delta S_{OO} \tag{5}$$

(2) Assuming no heat loss during the heat exchange process, according to the law of energy conservation, the heat exchange amount between the low-temperature heat source segment *XZ* and the working fluid segment *DH* is equal. Through this relationship, the flow rate of the working fluid can be calculated. Specifically, the heat released by the low-temperature heat source in segment *XZ* is entirely absorbed by the working fluid in segment *DH*, raising the temperature of the working fluid and evaporating it into gas. The flow rate of the working fluid can be calculated using the following formula:

$$l_d = \frac{z_{oh} l_h \left(S_X - S_Z\right)}{\left(g_H - g_D\right)} \tag{6}$$

(3) Similarly, according to energy conservation, the heat exchange amount between the low-temperature heat source segment *XZ* and the working fluid segment *DH* is equal. Through this energy balance relationship, the outlet temperature of the working fluid can be calculated. This process ensures that the residual heat of the heat source can be fully utilized by the working fluid, improving the thermal efficiency of the system. The outlet temperature of the exhaust can be calculated using the following formula:

$$S_F = S_Z - \frac{l_d \left(g_D - g_R\right)}{z_{oh} l_h} \tag{7}$$

(4) According to the above steps, the temperature differences between segments *FR*, *ZD*, and *XH* are calculated, and these temperature differences are compared with the minimum temperature difference ΔS_{oo}. Assuming that the minimum temperature difference ΔS_{oo} indeed occurs at the initially set saturation point *D*, the original assumption is valid, and the results are output. If other temperature differences are smaller than ΔS_{oo}, the point needs to be reset as the minimum temperature difference point, and the thermodynamic parameters of each part are recalculated according to the heat exchange balance method

In the low-temperature thermal cycle system for construction waste based on the Rankine cycle, construction waste acts as a low-temperature heat source, with a relatively low and potentially highly fluctuating heat source temperature. Therefore, the above modeling method ensures that the system can maintain high efficiency and stability under different operating conditions. The application of the pinch point temperature difference analysis method optimizes the heat exchange process by reasonably setting and adjusting the temperature differences at each point, reducing energy loss, and further improving the overall thermal efficiency of the system.

3.2 Mathematical model of the Rankine bottom cycle

Compared with traditional Rankine cycle systems, the model design of a low-temperature thermal cycle system based on construction waste needs to pay special attention to the characteristics of the low-temperature heat source. As a low-temperature heat source, construction waste has a relatively low and potentially highly fluctuating temperature, which requires special consideration in designing each component to maximize the use of the low-temperature heat source and ensure efficient operation of the system under different working conditions. In the entire system, the key is to optimize the heat exchange process so that the working fluid can fully absorb the residual heat from construction waste and efficiently convert it into mechanical or electrical energy. The low-temperature thermal cycle system based on the Rankine cycle primarily includes four key components: the working fluid pump, evaporator, expander, and condenser.

Specifically, the working fluid pump compresses and pressurizes the working fluid from a low-pressure liquid state to a high-pressure liquid state. This process consumes energy provided by electricity, and the pump's efficiency affects the system's overall efficiency. Therefore, during the design process, a high-efficiency working fluid pump should be selected to reduce energy consumption and improve the system's overall efficiency. Assuming the output power is denoted by *Q*, heat by *W*, mass flow rate of the working fluid by *l*, specific enthalpy of the working fluid by *g*, efficiency by λ, and the subscripts *o*, *EV*, *CO*, *s*, *h*, *FR*, *d*, and *r* represent the working fluid pump, evaporator, condenser, expander, generator, diesel engine, fuel oil, and exhaust gas, respectively, the efficiency of the pump is represented by λ_o, the power consumed by the pump can be calculated using the following formula:

$$\dot{Q}_o = \dot{l}_d \left(g_2 - g_1\right) / \lambda_o \tag{8}$$

The evaporator is a crucial heat exchange equipment in the system. In the evaporator, the working fluid absorbs residual heat from construction waste during isobaric heating, transforming from a liquid to high-temperature, high-pressure steam. The design of the evaporator should ensure that the low-temperature heat source from construction waste is fully utilized to maximize the heat absorbed by the working fluid. This requires optimizing the heat exchange area and efficiency of the evaporator to ensure the efficient operation of the system. The heat absorbed by the working fluid during isobaric heating can be calculated using the following formula:

$$W_{EV} = \dot{l}_d \left(g_3 - g_2\right) \tag{9}$$

The expander is the key equipment that converts the thermal energy of high-temperature, high-pressure steam into mechanical energy. After entering the expander, the high-temperature, high-pressure steam expands and does work, driving the generator coaxially connected to it to produce electricity. The performance of the expander directly affects the system's output power and net output power, so a high-efficiency expander is needed to improve the system's energy conversion efficiency, ensuring that the working fluid can release the maximum amount of energy during the expansion process. The output power and net output power of the expander can be calculated using the following formulas:

$$\dot{Q} = \dot{l}_d (g_3 - g_4) \lambda_s \lambda_h \tag{10}$$

$$\dot{Q}_{NET} = \dot{Q} - \dot{Q}_o \tag{11}$$

The condenser is responsible for condensing the expanded steam into liquid. In the condenser, the working fluid releases heat through isobaric heat exchange with the cold source, lowering its temperature and condensing into liquid. The heat exchange efficiency of the condenser and the temperature of the cold source are key factors affecting system performance. Optimizing the condenser design to ensure efficient condensation of the working fluid is crucial for improving the system's overall performance. The energy released by the working fluid during isobaric condensation in the condenser can be calculated using the following formula:

$$W_{CO} = \dot{l}_d (g_4 - g_1) \tag{12}$$

The low-temperature thermal cycle system model based on the Rankine cycle can be comprehensively evaluated through power analysis. This process includes analyzing each component individually and assessing the overall system's synergistic operation. In the context of construction waste as a low-temperature heat source, these analysis steps are particularly important because they help identify and optimize key energy utilization aspects. The work capacity of unit mass exhaust gas reflects the system's efficiency in utilizing the energy of the exhaust gas. Specifically, the work capacity of unit mass exhaust gas refers to the ratio of net output power to the mass of the exhaust gas. Through this analysis, the conversion efficiency of residual heat from construction waste in the system can be evaluated. The calculation formula is as follows:

$$O_{NET} = \dot{Q}_{NET} / \dot{l}_r \tag{13}$$

The power consumption factor represents the pump power consumed per unit expansion work, i.e., the efficiency of the pump power. Analyzing the power consumption factor can evaluate the efficiency of the working fluid pump and identify ways to reduce pump power consumption.

$$OZD = \dot{Q}_o / \dot{Q}_s \tag{14}$$

The volumetric flow rate ratio of the expander is an important parameter measuring the specific volume change of the working fluid during the expansion process. A lower volumetric flow rate ratio generally provides higher turbine efficiency. Therefore, in the low-temperature thermal cycle system for construction waste, the expander design needs to be optimized to maintain an efficient expansion process while handling low-temperature working fluid, improving the system's overall energy conversion efficiency.

$$NDE = \dot{N}_4 / \dot{N}_3 \tag{15}$$

Assuming the isentropic enthalpy drop through the expander is denoted by ΔG_{IS}, the formula for calculating the expander size parameter is:

$$TO = \sqrt{\dot{N}_4} \; / \; \Delta G_{IS}^{1/4} \tag{16}$$

The thermal efficiency of the Rankine cycle is:

$$\lambda = \frac{\dot{Q}_{NET}}{W_{EVA}} \tag{17}$$

The energy efficiency of the construction waste system can be calculated using the following formula:

$$\eta_{FR} = \dot{Q}_{FR} / \dot{W}_d \tag{18}$$

The thermal efficiency of the low-temperature thermal cycle system based on the Rankine cycle for construction waste is the combined efficiency of the construction waste residual heat recovery system and the main energy conversion system.

$$\lambda_{FR-QGE} = (O_{FR} + Q_{NET}) / \dot{W}_d \tag{19}$$

Further, exergy efficiency analysis of the low-temperature thermal cycle system model based on the Rankine cycle for construction waste is conducted. Before establishing the exergy of each component, the exergy of the working fluid at any point u in the system needs to be defined. The exergy of the working fluid represents the useful energy of the working fluid in a specific state, considering its internal energy, kinetic energy, potential energy, etc., and is calculated relative to the environmental reference state. In the low-temperature thermal cycle system for construction waste, special attention needs to be paid to the characteristics of the low-temperature heat source to ensure that the definition of the working fluid exergy accurately reflects the utilization of residual heat from construction waste. Assuming the exergy value is denoted by R, the specific entropy of the working fluid by t, loss by U, and the subscripts 0, IN, and OUT represent the environmental state, input, and output, respectively, the definition formula is as follows:

$$\dot{R}_u = \dot{l}_d [(g_u - g_0) - S_0 (t_u - t_0)] \tag{20}$$

Since there are always some irreversible factors in the actual process, any irreversible process will result in energy loss. The irreversibility of each component can be represented by exergy loss. In the system, the irreversibility of key components such as the working fluid pump, evaporator, expander, and condenser needs to be analyzed separately. For example, friction loss and flow loss may occur during the compression process of the working fluid pump, and incomplete heat transfer may occur during the heat exchange process of the evaporator. Such irreversibility needs to be calculated and evaluated in detail, and the irreversibility of each component can be expressed as:

$$\dot{U}_u = \sum \dot{R}_{IN} - \sum \dot{R}_{OUT} - \dot{Q}_u \tag{21}$$

The total irreversibility of the cycle system is the sum of the irreversibility of each component in the system. By calculating the total irreversibility of the system, the energy loss points in the system operation process can be identified, and possible optimization directions can be found. For the low-temperature thermal cycle system for construction waste, special attention needs to be paid to the loss during the transfer of low-temperature residual heat to ensure maximum utilization of these low-temperature heat sources.

$$\dot{U}_{QGE} = \sum \dot{U}_u \tag{22}$$

The exergy loss factor represents the system's irreversibility caused by generating unit net power and explains the system's perfection and the working fluid's work capacity. A lower exergy loss factor means the system is closer to the ideal state, and the working fluid can be more efficiently converted into useful work. In the construction waste system, analyzing the exergy loss factor can identify key factors affecting system performance, such as the efficiency of the working fluid pump and the heat exchange performance of the evaporator, and optimize them accordingly.

$$RFD = \dot{U}_{QGE} / \dot{Q}_{NET} \tag{23}$$

High exergy efficiency means that the system can efficiently utilize the low-temperature residual heat from construction waste, converting it into useful work or other forms of energy. For the low-temperature thermal cycle system for construction waste, calculating the system's exergy efficiency can evaluate the effectiveness of residual heat utilization and further optimize system design to improve overall performance.

$$\lambda_r = \dot{Q}_{NET} / E_{IN} \tag{24}$$

Through the above exergy efficiency analysis steps, the thermodynamic performance of the low-temperature thermal cycle system model based on the Rankine cycle for construction waste can be comprehensively evaluated. This process includes analyzing each component individually and assessing the overall system's synergistic operation. Especially in the utilization of low-temperature residual heat, optimizing the design and operating parameters of each link can maximize the recovery and efficient utilization of residual heat from construction waste.

4. EXPERIMENTAL RESULTS AND ANALYSIS

In the experiment, thermogravimetric analysis was performed on two different ratios of construction waste samples, namely wood waste 40% + plastic waste 30% + rubber waste 30% (sample 1) and wood waste 70% + plastic waste 20% + rubber waste 10% (sample 2). It can be known from Figure 5, Sample 1 reduced to 70% of its mass at 200°C, indicating that the initial rapid weight loss was mainly due to the decomposition of wood and plastic. Subsequently, at 400°C and 600°C, the mass remained almost unchanged at 70% and 68%, respectively, indicating a slower decomposition rate during this stage. However, at 800°C, the mass rapidly decreased to 20%, showing that rubber began to decompose significantly, and finally, the mass reduced to 10% at 1000°C. In contrast, sample 2 reduced to 70% of its mass at 200°C, and at 400°C and 600°C, the mass was 68% and 50%, respectively, indicating that the higher proportion of wood in this sample made the decomposition process slower. Particularly, the mass decreased to 20% at 800°C and remained at 10% at 1000°C. By comparing the mass change rates at different temperatures, it can be found that sample 1 had a faster decomposition rate at 800°C (-0.45), while sample 2 had a faster decomposition rate at 600°C (-0.65), showing the differences in pyrolysis characteristics under different ratios of components.

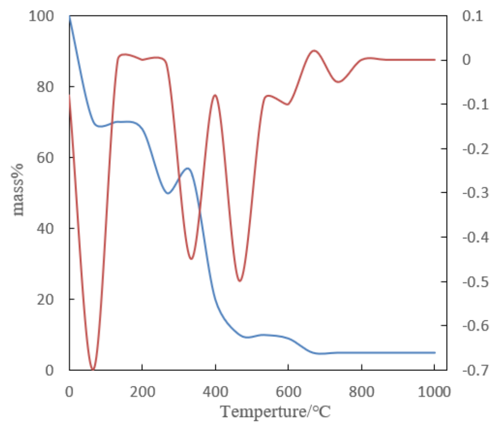

1) Wood Waste 40% + Plastic Waste 30% + Rubber Waste 30%

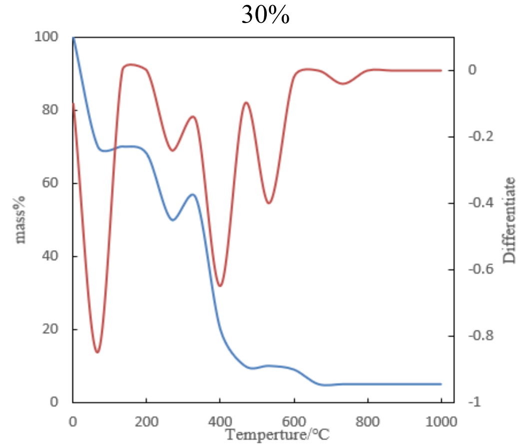

2) Wood Waste 70% + Plastic Waste 20% + Rubber Waste 10%

Figure 5. Thermogravimetric curves of construction waste samples

By comparing the thermogravimetric curves of the two different ratios of construction waste samples, the key influencing factors of the pyrolysis reaction mechanism can be concluded. In sample 1, the higher proportion of plastic and rubber significantly accelerated the decomposition rate in the high-temperature stage (800°C and 1000°C), especially the significant mass reduction at 800°C indicating the main decomposition stage of rubber. In sample 2, due to the higher proportion of wood, the decomposition process was relatively more stable, showing significant mass reduction mainly due to wood decomposition in the medium temperature stage (600°C). This result reveals the distinct differences in decomposition temperatures and rates of various components in construction waste with different ratios. Wood primarily decomposes in the medium temperature stage, while plastic and rubber decompose more intensely at higher temperatures. This study demonstrates the pyrolysis reaction mechanism of construction waste through experimental data, effectively proving the impact of different component ratios on pyrolysis characteristics, providing a scientific basis for subsequent thermodynamic performance analysis. This analysis method not only reveals the key reaction mechanisms during the pyrolysis process of construction waste but also provides strong support for optimizing waste resource utilization in practical engineering applications.

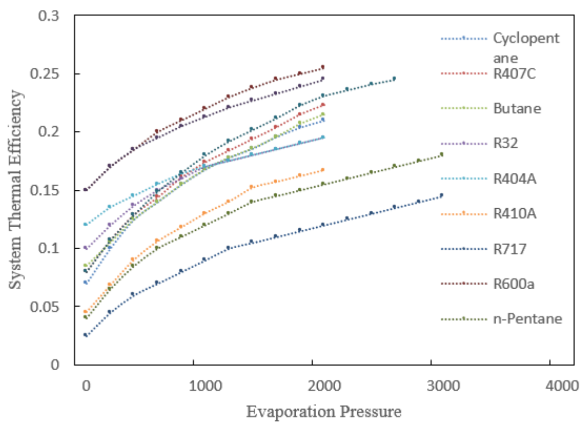

Figure 6. System thermal efficiency

By experimentally analyzing the evaporation pressure of different working fluids in the low-temperature thermal cycle system for construction waste, the thermal efficiency changes of each working fluid under different pressures can be observed. According to Figure 6, for Cyclopentane, its thermal efficiency gradually increases from 0.07 to 0.21, showing a relatively stable growth within the pressure range of 0 to 3000 kPa. Similarly, R407C and Butane also show similar growth trends within the same pressure range, with thermal efficiencies increasing from 0.08 to 0.223 and 0.085 to 0.215, respectively. R32 and R404A, on the other hand, start with higher initial thermal efficiencies (0.1 and 0.12) and gradually increase to 0.195. R410A has the lowest initial thermal efficiency, only 0.045, but increases to 0.167 under high pressure, showing a significant increase. In contrast, R717 has a lower initial thermal efficiency (0.025), but its growth is stable, reaching 0.145 under high pressure. R600a and Isopentane start with relatively high initial thermal efficiencies (0.15) and gradually increase to 0.255 and 0.245, respectively, showing significant thermal efficiency advantages. Other working fluids such as n-Pentane and R152a also exhibit similar growth trends, especially R152a, which achieves a high thermal efficiency of 0.245 under high pressure.

By comparing the thermal efficiency data of different working fluids in the low-temperature thermal cycle system for construction waste, the performance differences and advantages of different working fluids within a specific pressure range can be observed. Working fluids with high initial thermal efficiencies, such as R32 and R404A, already exhibit high thermal efficiencies under relatively low-pressure conditions, making them suitable for operation under relatively low-pressure conditions. Although R410A has a low initial thermal efficiency, it shows the greatest increase under high pressure, making it suitable for systems requiring a wide range of pressure adjustments. Although R717 and n-Pentane have lower initial thermal efficiencies, their stable growth trends make them also have application potential under specific conditions. Particularly, R600a and Isopentane show high thermal efficiencies across the entire pressure range, demonstrating their advantages in low-temperature thermal cycle systems.

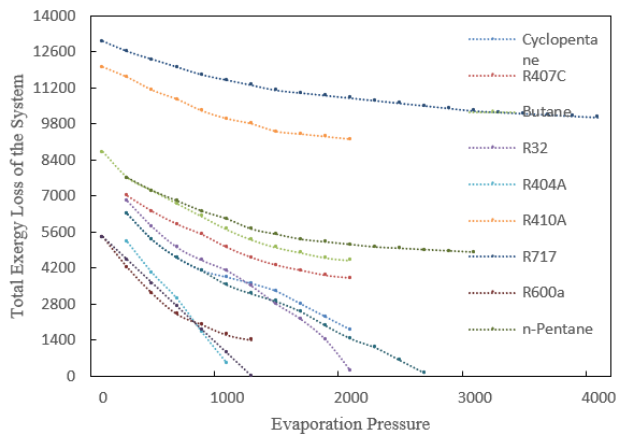

Figure 7. Total exergy loss of the system

Through the analysis of the total exergy loss of different working fluids in the low-temperature thermal cycle system for construction waste, the results show significant differences in exergy loss at different evaporation pressures. According to Figure 7 and taking Cyclopentane as an example, its total exergy loss gradually decreases from 6300 to 1800 as the evaporation pressure increases from 0 to 4000 kPa, showing a trend of decreasing exergy loss with increasing pressure. R407C decreases from 7000 to 3800, showing a similar decreasing trend but with higher overall exergy loss values. Butane's total exergy loss decreases from 8700 to 4500 between 0 and 4000 kPa, showing relative stability at high pressure. R32 and R404A exhibit a sharp decline in total exergy loss at high pressure, dropping from 6800 and 5200 to 200 and 500, respectively. Although R410A has an initial total exergy loss as high as 12000, it maintains a lower exergy loss level under high pressure, gradually decreasing to 9200. In contrast, R717 has relatively low total exergy loss across the pressure range, gradually decreasing from 13000 to 10050. Other working fluids like R600a and Isopentane also show significant reductions in total exergy loss at high pressure, decreasing from 5400 and 5400 to 1400 and 0, respectively. n-Pentane and R152a show a stable decreasing trend, decreasing from 7700 and 6300 to 4800 and 100.

Through detailed comparative analysis of the total exergy loss of different working fluids in the low-temperature thermal cycle system for construction waste, the differences in thermal performance under different pressure conditions can be concluded. Although Cyclopentane and R407C have higher initial total exergy loss, they show significant reductions in exergy loss under high pressure, indicating good thermodynamic performance under high-pressure conditions. Butane and R32 have significant decreases in exergy loss across the entire pressure range, especially R32, which has the lowest exergy loss under high pressure, showing its superiority under high-pressure conditions. Although R410A and R717 have high initial total exergy loss, they maintain lower exergy loss levels under high pressure, making them suitable for systems requiring a wide range of pressure adjustments. R600a and Isopentane show significant reductions in total exergy loss under high pressure, especially Isopentane, which has an exergy loss of 0 at 4000 kPa, demonstrating its excellent thermodynamic performance. n-Pentane and R152a show stable decreases in exergy loss across the entire pressure range, making them suitable for operation under medium to high pressure conditions.

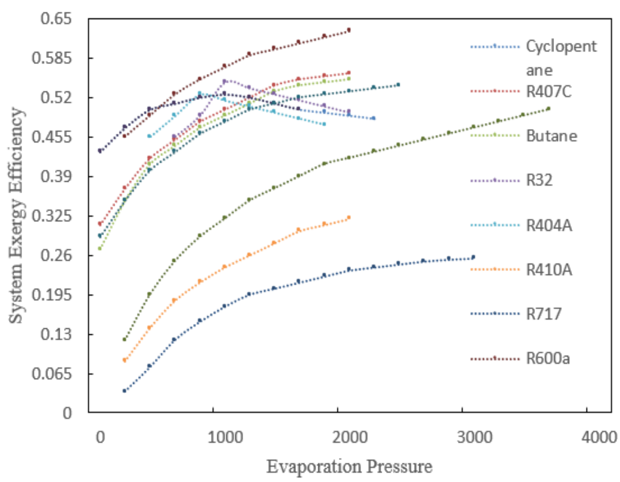

Figure 8. System exergy efficiency

By analyzing the exergy efficiency of different working fluids in the low-temperature thermal cycle system for construction waste, the changes in exergy efficiency at different evaporation pressures can be observed. As can be seen in Figure 8, cyclopentane's exergy efficiency gradually increases from 0.43 at 0 kPa to 0.52 at 1000 kPa, then slightly decreases to 0.485, showing the highest efficiency at moderate pressure. R407C's exergy efficiency gradually increases from 0.31 to 0.56 within the evaporation pressure range of 0 to 4000 kPa, showing a continuous and stable growth trend. Butane's exergy efficiency increases from 0.27 to 0.55 within the same pressure range, showing a high efficiency level. R32 and R404A reach the highest efficiency at 2000 kPa, 0.545 and 0.525 respectively, then slightly decrease. R410A's exergy efficiency increases significantly from 0.085 to 0.32 within the pressure range of 0 to 4000 kPa. In contrast, R717's exergy efficiency increases significantly from 0.035 to 0.255 within the same pressure range. R600a shows continuous growth across the entire pressure range, with exergy efficiency increasing from 0.455 to 0.63. n-Pentane and Isopentane also show significant growth in exergy efficiency at high pressure, increasing from 0.12 and 0.43 to 0.5, respectively. R152a's exergy efficiency increases from 0.29 to 0.54, showing a stable growth trend.

By analyzing the exergy efficiency data of different working fluids in the low-temperature thermal cycle system for construction waste, the differences in thermal performance under different pressure conditions can be observed. Cyclopentane and R407C show higher exergy efficiency at moderate pressure, especially R407C, which reaches 0.56 under high pressure, demonstrating its excellent thermodynamic performance. Butane also shows high exergy efficiency across the entire pressure range, especially reaching 0.55 under high pressure, making it suitable for operation under high-pressure conditions. R32 and R404A show high exergy efficiency under medium to high pressure conditions, making them suitable for applications within this pressure range. Although R410A has low initial exergy efficiency, it shows significant growth under high pressure, making it suitable for systems requiring a wide range of pressure adjustments. Although R717 has low initial exergy efficiency, it shows significant growth under high pressure, making it suitable for operation under high-pressure conditions. R600a and n-Pentane show continuous efficiency growth across the entire pressure range, especially R600a, which reaches 0.63 under high pressure, demonstrating excellent thermodynamic performance. Isopentane and R152a also show high exergy efficiency under high pressure, reaching 0.5 and 0.54, respectively.

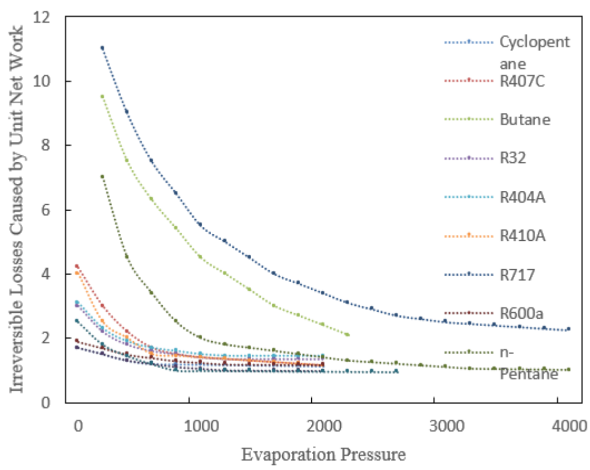

Figure 9. Irreversible losses caused by unit net work

By analyzing the irreversible losses caused by unit net work of different working fluids in the low-temperature thermal cycle system for construction waste, the changes in irreversible losses under different evaporation pressures can be observed. It can be seen from Figure 9, that cyclopentane's irreversible losses decrease from 1.7 at 0 kPa to 1.13 at 3000 kPa, showing a trend of decreasing irreversible losses with increasing evaporation pressure. R407C's irreversible losses decrease from 4.2 to 1.15, showing a significant downward trend. Butane's irreversible losses decrease from 9.5 to 2.1 within the range of 0 to 3000 kPa, showing a significant reduction. R32's irreversible losses decrease from 3.0 to 1.35 and stabilize after 2000 kPa. R404A's irreversible losses decrease from 3.1 to 1.45 and remain stable after 2000 kPa. R410A's irreversible losses decrease from 4.0 to 1.15, showing a continuous downward trend. R717's irreversible losses decrease significantly from 11 to 2.5 within the range of 0 to 3000 kPa. R600a's irreversible losses decrease from 1.9 to 1.18, showing a relatively small but stable downward trend. n-Pentane's irreversible losses decrease significantly from 7 to

1.1. Isopentane's irreversible losses decrease from 1.7 to 0.98, and R152a's decrease from 2.5 to 0.96, both showing significant downward trends.

Through detailed analysis of the irreversible losses caused by unit net work of different working fluids in the low-temperature thermal cycle system for construction waste, the differences in thermal performance under different pressure conditions can be seen. Cyclopentane and R407C show significant reductions in irreversible losses under high pressure, especially R407C, which decreases from 4.2 to 1.15, showing excellent thermodynamic performance under high-pressure conditions. Butane shows significant reductions in irreversible losses across the entire pressure range, especially from 9.5 to 2.1 under high pressure, making it suitable for operation under high-pressure conditions. R32 and R404A's irreversible losses stabilize after 2000 kPa, showing their advantages in the medium-high pressure range. R410A's irreversible losses decrease significantly across the entire pressure range, making it suitable for systems requiring wide pressure adjustments. R717's irreversible losses decrease significantly from 11 to 2.5 under high pressure, making it suitable for operation under high-pressure conditions. R600a and n-Pentane show continuous efficiency growth across the entire pressure range, especially n-Pentane, which decreases to 1.1 under high pressure, showing excellent thermodynamic performance. Isopentane and R152a's irreversible losses are also low under high pressure, reaching 0.98 and 0.96, respectively.

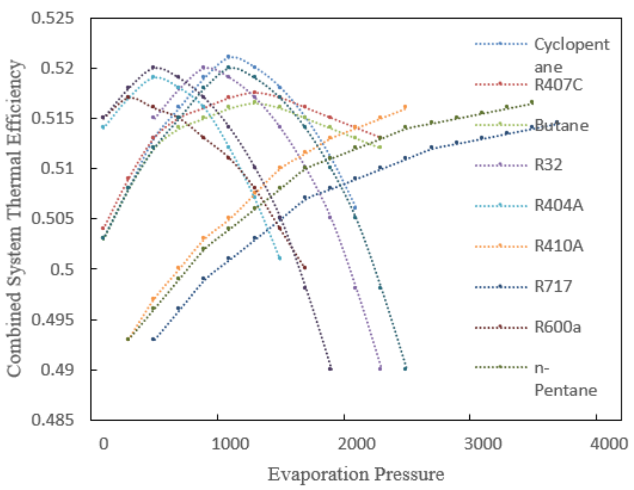

Figure 10. Combined system thermal efficiency

By analyzing the thermal efficiency of different working fluids in the combined low-temperature thermal cycle system for construction waste, the changes in thermal efficiency under different evaporation pressures can be observed. According to Figure 10, cyclopentane's thermal efficiency gradually increases from 0.503 at 0 kPa to 0.506 at 3000 kPa, showing slight growth and a stable trend with increasing pressure. R407C's thermal efficiency increases significantly from 0.504 at 0 kPa to 0.514 at 3000 kPa. Butane's thermal efficiency increases from 0.503 at 0 kPa to 0.512 at 3000 kPa, showing a stable growth trend. R32 reaches its maximum thermal efficiency of 0.518 at 1000 kPa, then gradually decreases to 0.49 at 3000 kPa with increasing pressure. R404A's thermal efficiency reaches 0.517 at 1000 kPa, then gradually decreases to 0.501. R410A's thermal efficiency gradually increases from 0.493 at 1000 kPa to 0.516 at 3000 kPa, showing significant growth. R717's thermal efficiency gradually increases from 0.493 at 1000 kPa to 0.513 at 3000 kPa, showing continuous growth. R600a's thermal efficiency gradually decreases from 0.515 at 0 kPa to 0.5 at 3000 kPa with increasing pressure. n-Pentane's thermal efficiency gradually increases from 0.493 at 1000 kPa to 0.5155 at 3000 kPa, showing significant growth. Isopentane's thermal efficiency reaches 0.518 at 1000 kPa, then gradually decreases to 0.49 at 3000 kPa. R152a's thermal efficiency gradually increases from 0.503 at 0 kPa to 0.52 at 1000 kPa, then gradually decreases to 0.49 at 3000 kPa with increasing pressure.

Through detailed analysis of the thermal efficiency data of different working fluids in the combined low-temperature thermal cycle system for construction waste, the differences in thermal performance under different pressure conditions can be seen. Cyclopentane and R407C show significant thermal efficiency improvements under high pressure, especially R407C, which increases from 0.504 to 0.514, showing excellent thermodynamic performance under high-pressure conditions. Butane shows stable growth in thermal efficiency across the entire pressure range, especially reaching 0.512 under high pressure, making it suitable for operation under high-pressure conditions. R32 and R404A's thermal efficiency decreases with increasing pressure after reaching their highest thermal efficiency, indicating their advantages under moderate pressure conditions. R410A's thermal efficiency increases significantly across the entire pressure range, from 0.493 to 0.516, making it suitable for systems requiring wide pressure adjustments. R717's thermal efficiency increases significantly from 0.493 to 0.513 under high pressure, making it suitable for operation under high-pressure conditions. R600a's thermal efficiency gradually decreases across the entire pressure range, indicating its excellent performance under low-pressure conditions. n-Pentane shows significant thermal efficiency improvement under high pressure, increasing from 0.493 to 0.5155, showing excellent thermodynamic performance. Isopentane and R152a also show improvements in thermal efficiency under high pressure but decrease with further pressure increase.

5. CONCLUSION

The main content of this paper is divided into two parts: first, the pyrolysis reaction mechanism of construction waste was analyzed through experiments and simulations, revealing the decomposition patterns and reaction mechanisms of various components during pyrolysis; second, the thermodynamic performance of the low-temperature thermal cycle system for construction waste was analyzed, evaluating its energy utilization efficiency and economic benefits, and exploring its feasibility and application prospects in practical engineering. The experimental results include: thermogravimetric curves of construction waste samples, showing mass changes at different temperatures; system thermal efficiency and combined system thermal efficiency, evaluating the thermal performance of single working fluid and combined working fluid systems respectively; total exergy loss and exergy efficiency of the system, quantifying energy losses and energy utilization efficiency during system operation; and irreversible losses caused by unit net work, analyzing the changes in irreversible losses of different working fluids under different evaporation pressures.

This paper revealed the decomposition patterns and reaction mechanisms of various components during the pyrolysis process and provides a scientific basis for the selection of working fluids and system optimization in practical engineering applications through detailed studies on the pyrolysis reaction mechanism of construction waste and the thermodynamic performance of the low-temperature thermal cycle system. The experimental results show significant differences in thermal performance of different working fluids under different pressure conditions, with Cyclopentane, R407C, and Butane showing excellent thermal performance under high pressure, while R410A and R717 show high thermal efficiency and low irreversible losses across the entire pressure range. This study not only helps improve the energy utilization efficiency of the system but also provides important theoretical support for exploring new ways of resource utilization of construction waste.

The study provides a scientific basis for the pyrolysis reaction mechanism and the optimization design of the low-temperature thermal cycle system for construction waste, having important theoretical and engineering application value. However, there are certain limitations in the selection of working fluids and system design. Future research should further expand the variety of working fluids and verify them in practical engineering applications. In addition, considering the complexity and diversity of construction waste components, future research should focus on the pyrolysis reaction mechanism analysis of multi-component systems and the optimization of system thermodynamic performance under different operating conditions. Through further research and experimental verification, more efficient and economical engineering applications for resource utilization of construction waste are expected to be achieved.

REFERENCES

[1] Kontokosta, C.E., Hong, B., Johnson, N.E., Starobin, D. (2018). Using machine learning and small area estimation to predict building-level municipal solid waste generation in cities. Computers, Environment and Urban Systems, 70: 151-162. https://doi.org/10.1016/j.compenvurbsys.2018.03.004

[2] Voicu, G., Toma, M.L., Tudor, P., Ipate, G., Ştefan, V. (2018). Aspects regarding the compression resistance of geosynthetics used in building municipal solid waste landfills. INMATEH - Agricultural Engineering, 54(1): 7-14. http://www.inmateh.eu/INMATEH_1_2018/INMATEH-Agricultural_Engineering_54_2018.pdf.

[3] Bruyako, M., Grigoryeva, L. (2018). Ecologically safe composite building materials based on cellulose-containing solid household waste. In MATEC Web of Conferences, 193: 02007. https://doi.org/10.1051/matecconf/201819302007

[4] Gowda, S., Kunjar, V., Gupta, A., Havanagi, V.G., Kavitha, G. (2023). Municipal incinerated solid waste bottom ash as sustainable construction material in the construction of flexible pavements. Journal of Material Cycles and Waste Management, 25(6): 3824-3833. https://doi.org/10.1007/s10163-023-01809-2

[5] Naser, S.S.M., Seyedi, M., Al-busaltan, S. (2023). Enhancing Stone Mastic Asphalt through the Integration of waste paper and Cement Kiln Dust. Journal of Civil and Hydraulic Engineering, 1(1): 23-37. https://doi.org/10.56578/jche010103

[6] Zhang, X., Xing, J., Gao, Z., Zhang, H. (2022). Evaluation method of solid construction waste recycling capacity based on AHP-fuzzy algorithm. International Journal of Environmental Technology and Management, 25(4): 273-284. https://doi.org/10.1504/IJETM.2022.124415

[7] Chen, Y., Zhao, M., Lv, Y., Ting, Z. J., Zhao, S., Liu, Z.B., Zhang, X., Yang, Y.D., You, Y., Yuan, W. (2023). Utilization of municipal solid waste incineration fly ash as construction materials based on geopolymerization. Resources, Conservation & Recycling Advances, 19: 200162. https://doi.org/10.1016/j.rcradv.2023.200162

[8] Yu, H., Zahidi, I., Liang, D. (2023). Sustainable porous-insulation concrete (SPIC) material: Recycling aggregates from mine solid waste, white waste and construction waste. Journal of Materials Research and Technology, 23: 5733-5745. https://doi.org/10.1016/j.jmrt.2023.02.181

[9] Sakurai, Y., Sugimura, E., Ito, T., Harada, H. (2024). Product characteristics and heat of reaction of municipal solid waste in pyrolysis and gasification at low temperatures. Journal of Material Cycles and Waste Management, 26(3): 1418-1431. https://doi.org/10.1007/s10163-024-01900-2

[10] Li, J., Yang, X., Hou, L., Yan, B., Cheng, Z., Zhao, J., Chen, G. (2024). Pyrolysis-combustion of rural solid waste: Self-sustaining operation and pollutants emission. Fuel, 368: 131575. https://doi.org/10.1016/j.fuel.2024.131575

[11] Marchetti, L., Guastaferro, M., Annunzi, F., Tognotti, L., Nicolella, C., Vaccari, M. (2024). Two-stage thermal pyrolysis of plastic solid waste: Set-up and operative conditions investigation for gaseous fuel production. Waste Management, 179: 77-86. https://doi.org/10.1016/j.wasman.2024.03.011

[12] Feng, S., Feng, Y., Ji, L., Zhan, M., Wang, J., Xu, X. (2024). Distribution of gasification products and emission of heavy metals and dioxins from municipal solid waste at the low temperature pyrolysis stage. Environmental Science and Pollution Research, 31(11): 16388-16400. https://doi.org/10.1007/s11356-024-32284-3

[13] Zheng, Y., Li, A., Huang, Y., Zhang, T., Usman, M., Bie, N., Yao, H. (2023). Application of bp neural network in pyrolysis treatment of organic solid waste. In International Symposium on Water Pollution and Treatment, Cham: Springer Nature Switzerland, pp. 191-204. https://doi.org/10.1007/978-3-031-53456-0_16

[14] Urciuolo, M., Migliaccio, R., Chirone, R., Bareschino, P., Mancusi, E., Pepe, F., Ruoppolo, G. (2023). Thermal and catalytic pyrolysis of real plastic solid waste as a sustainable strategy for circular economy. Combustion Science and Technology, 195(14): 3426-3439. https://doi.org/10.1080/00102202.2023.2239449

[15] Li, L., Chen, J. (2024). Quantification of tiny damage variation in asphalt mixture during the low-temperature thermal cycle. Construction and Building Materials, 411: 134266. https://doi.org/10.1016/j.conbuildmat.2023.134266

[16] Daniarta, S., Nemś, M., Kolasiński, P. (2023). A review on thermal energy storage applicable for low-and medium-temperature organic Rankine cycle. Energy,

127931. https://doi.org/10.1016/j.energy.2023.127931
[17] Almatrafi, E., Moloney, F., Goswami, D.Y. (2022). Mechanical Vapor Compression. Journal of Solar Energy Engineering, Transactions of the ASME.
[18] Pfadt-Trilling, A. R., Widyolar, B. K., Jiang, L., Brinkley, J., Bhusal, Y., Winston, R., Fortier, M. O. P. (2023). Life cycle greenhouse gas emissions of low-temperature process heat generation by external compound parabolic concentrator (XCPC) solar thermal array. Renewable Energy, 205: 992-998. https://doi.org/10.1016/j.renene.2023.01.117
[19] Daniarta, S., Nemś, M., Kolasiński, P., Pomorski, M. (2022). Sizing the thermal energy storage device utilizing phase change material (PCM) for low-temperature organic Rankine cycle systems employing selected hydrocarbons. Energies, 15(3): 956. https://doi.org/10.3390/en15030956
[20] Koen, A., Farres-Antunez, P., Macnaghten, J., White, A. (2021). A low-temperature glide cycle for pumped thermal energy storage. Journal of Energy Storage, 42: 103038. https://doi.org/10.1016/j.est.2021.103038